

# Discovering objects and their localization in images

ICCV 2005 Paper number 1639

March 14, 2005

## Abstract

*We seek to discover the object categories depicted in a set of unlabelled images. We achieve this using a model developed in the statistical text literature: probabilistic Latent Semantic Analysis (pLSA). In text analysis this is used to discover topics in a corpus using the bag-of-words document representation. Here we discover topics as object categories, so that an image containing instances of several categories is modeled as a mixture of topics.*

*The model is applied to images by using a visual analogue of a word, formed by vector quantizing SIFT-like region descriptors. The topic discovery approach successfully translates to the visual domain: for a small set of objects, we show that both the object categories and their approximate spatial layout are found without supervision.*

*We also demonstrate classification of new images and of images containing multiple objects. Performance of the proposed unsupervised method is compared to the supervised approach of [6] on a set of images containing only one object per image, and also compared with the ground truth labeling on a set of images containing multiple objects per image. These results demonstrate that we can successfully build object class models from an unsupervised analysis of images.*

## 1. Introduction

Common approaches to object recognition involve some form of supervision. This may range from specifying the object's location and segmentation, as in face detection [14, 19], to providing only auxiliary data indicating the object's identity [1, 5, 6, 20]. For a large dataset, any annotation is expensive, or may introduce unforeseen biases. Results in speech recognition and machine translation highlight the importance of huge amounts of training data. The quantity of good, unsupervised training data – the set of still images – is orders of magnitude larger than the visual data available with annotation. Thus, one would like to observe many images and infer models for the classes of visual objects contained within them *without* supervision. This motivates the scientific question which, to our knowledge, has not been convincingly answered before: Is it possible to learn visual object classes simply from looking at

images?

Given large quantities of training data there has been notable success in unsupervised topic discovery in text, and it is this success that we wish to build on. We apply models used in statistical natural language processing to discover object categories and their image layout analogously to topic discovery in text. In our setting, documents are images and we quantize local appearance descriptors to form visual “words” [4, 15, 16, 21]. The two models we have investigated are the probabilistic Latent Semantic Analysis (pLSA) of Hofmann [7, 8], and the Latent Dirichlet Allocation (LDA) of Blei *et al.* [3]. Each model consistently gave similar results and we focus our exposition in this paper on the simpler pLSA method. Both models use the ‘bag of words’ representation, where positional relationships between features are ignored. This greatly simplifies the analysis, since the data are represented by an observation matrix, a tally of the counts of each word (rows) in every document (columns).

The ‘bag of words’ model offers a rather impoverished representation of the data because it ignores any spatial relationships between the features. Nonetheless, it has been surprisingly successful in the text domain, because of the high discriminative power of some words and the redundancy of language in general. But can it work for objects, where the spatial layout of the features may be almost as important as the features themselves? While it seems implausible, there are several reasons for optimism: (i) as opposed to old corner detectors, modern feature descriptors have become powerful enough to encode very complex visual stimuli, making them quite discriminative; (ii) because visual features overlap in the image, some spatial information is implicitly preserved (i.e. randomly shuffling bits of the image around will almost certainly change the bag of words description). In this paper, we show that this optimism is not groundless.

While we ignore spatial position in our ‘bag of words’ object class models, our models are sufficiently discriminative to localize objects within each image, providing an approximate segmentation of each object topic from the other within an image. Thus, these bag-of-features models are a step towards top-down segmentation and spatial grouping.

We take this point on segmentation further by develop-

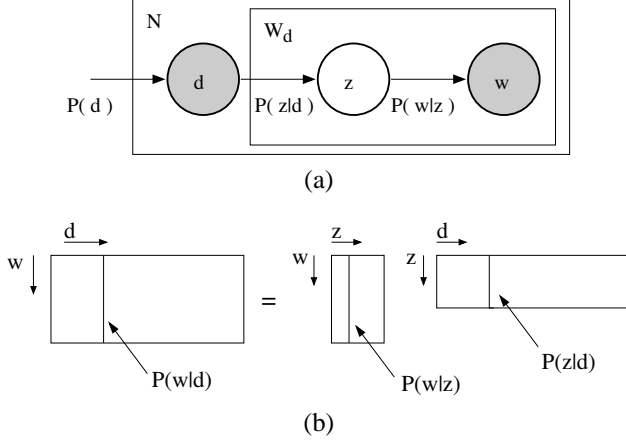


Figure 1: (a) pLSA graphical model, see text. Nodes inside a given box (plate notation) indicate that they are replicated the number of times indicated in the top left corner. Filled circles indicate observed random variables; unfilled are unobserved. (b) In pLSA the goal is to find the topic specific word distributions  $P(w|z_k)$  and corresponding document specific mixing proportions  $P(z|d_j)$  which make up the document specific word distribution  $P(w|d_j)$ .

ing a second vocabulary which is sensitive to the spatial layout of the words. This vocabulary is formed from spatially neighbouring word pairs, which we dub *doublets*. We demonstrate that doublets provide a cleaner segmentation of the various objects in each image. This means that both the object category and image segmentation are determined in an unsupervised fashion.

Sect. 2 describes the pLSA statistical model; various implementation details are given in Sect. 3. To explain and compare performance, in Sect. 4 we apply the models to sets of images for which the ground truth labeling is known. We also compare performance with a baseline model: a mixture model of Gaussian word distributions. Results are presented for object detection and segmentation. We summarize in Sect. 5.

## 2. The topic discovery model

We will describe the models here using the original terms ‘documents’ and ‘words’ as used in the text literature. Our visual application of these (as images and visual words) is then given in the following sections.

Suppose we have  $N$  documents containing words from a vocabulary of size  $M$ . The corpus of text documents is summarized in a  $M$  by  $N$  co-occurrence table  $N$ , where  $n(w_i, d_j)$  stores the number of occurrences of a word  $w_i$  in document  $d_j$ . This is the bag of words model. In addition, there is a hidden (latent) topic variable  $z_k$  associated with each occurrence of a word  $w_i$  in a document  $d_j$ .

**pLSA:** The joint probability  $P(w_i, d_j, z_k)$  is assumed to have the form of the graphical model shown in figure 1(a). Marginalizing over topics  $z_k$  determines the conditional probability  $P(w_i|d_j)$ :

$$P(w_i|d_j) = \sum_{k=1}^K P(z_k|d_j)P(w_i|z_k), \quad (1)$$

where  $P(z_k|d_j)$  is the probability of topic  $z_k$  occurring in document  $d_j$ ; and  $P(w_i|z_k)$  is the probability of word  $w_i$  occurring in a particular topic  $z_k$ .

The model (1) expresses each document as a convex combination of  $K$  topic vectors. This amounts to a matrix decomposition as shown in figure 1(b) with the constraint that both the vectors and mixture coefficients are normalized to make them probability distributions. Essentially, each document is modelled as a mixture of topics – the histogram for a particular document being composed from a mixture of the histograms corresponding to each topic.

Fitting the model involves determining the topic vectors which are common to all documents and the mixture coefficients which are specific for each document. The goal is to determine the model that gives high probability to the words that appear in the corpus, and a maximum likelihood estimation of the parameters is obtained by maximizing the objective function:

$$L = \prod_{i=1}^M \prod_{j=1}^N P(w_i|d_j)^{n(w_i, d_j)}, \quad (2)$$

where  $P(w_i|d_j)$  is given by (1).

This is equivalent to minimizing the Kullback-Leibler divergence between the measured empirical distribution  $\tilde{P}(w|d)$  and the fitted model. The model is fitted using the Expectation Maximization (EM) algorithm as described in [8].

**LDA:** In contrast to pLSA, LDA treats the multinomial weights over topics as latent random variables. The pLSA model is extended by sampling those weights from a Dirichlet distribution, the conjugate prior to the multinomial distribution. We consistently found similar performance with the two algorithms, and focus our description here on the simpler pLSA method. Reference [?] gives details of our LDA implementation and results, and [3] compares LDA with pLSA.

## 3. Implementation details

**Obtaining visual words:** We seek a vocabulary of visual words which will be insensitive to changes in viewpoint and illumination. To achieve this we use vector quantized SIFT descriptors [9] computed on affine covariant regions [10, 11, 13]. Affine covariance gives us tolerance to

viewpoint changes; SIFT descriptors, based on histograms of local orientation, give some tolerance to illumination change. Vector quantizing these descriptors gives tolerance to morphology within an object category. Others have used similar descriptors for object classification [4, 12], but in a supervised setting.

Two types of affine co-variant regions are computed for each image. The first is constructed by elliptical shape adaptation about an interest point. The method is described in [11, 13]. The second is constructed using the maximally stable procedure of Matas *et al.* [10] where areas are selected from an intensity watershed image segmentation. For both of these we use the binaries provided at [18]. Both types of regions are represented by ellipses. These are computed at twice the originally detected region size in order for the image appearance to be more discriminating.

Each ellipse is mapped to a circle by appropriate scaling along its principal axes and a SIFT descriptor is computed. There is no rotation of the patch. Alternatively, the SIFT descriptor could be computed relative to the the dominant gradient orientation within a patch, making the descriptor rotation invariant [9]. The SIFT descriptors are then vector quantized into the visual ‘words’ for the vocabulary. The vector quantization is carried out here by  $k$ -means clustering computed from about 300K regions. The regions are those extracted from a random subset (about one third of each category) of images of airplanes, cars, faces, motor-bikes and backgrounds (see experiment (2) in section 4). About 1K clusters are used for each of the Shape Adapted and Maximally Stable regions, and the resulting total vocabulary has 2,237 words. The number of clusters,  $k$ , is clearly an important parameter. The intention is to choose the size of  $k$  to determine words which give some intra-class generalization. This vocabulary is used for all the experiments throughout this paper.

In text, a word with two different meanings is called polysemous (e.g. ‘bank’ as in (i) a money keeping institution, or (ii) a river side). Of course, we observe the analogue of polysemy in our visual words, however, the topic discovery models can cope with these. A polysemous word would have a high probability in two different topics. The hidden topic variable associated with each word occurrence in a particular document can assign such a word to particular topic depending on the context of the document. We return to this point in section 4.3.

**Doublet visual words** [[\*\*\*\*\* make this better \*\*\*\*\*]] For the task of segmentation, we seek to increase the specificity of object description while at the same time allowing for configurational changes. We thus augment our vocabulary of words with “doublets”, pairs of visual words which co-occur within a local neighborhood. As candidate doublet words, we consider only the 200 words with high

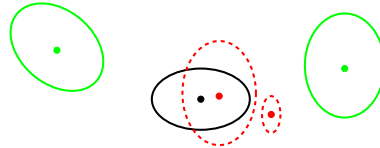


Figure 2: The doublet formation process. We wish to form doublets consisting of the two nearest neighbors with the word ellipse outlined in black. The two green ellipses are the resulting words that are used to form the doublets. The smaller red ellipse, while actually closer than the two green ellipses, is significantly smaller and consequently is not a nearest neighbor (after its distance is scaled by the scale ratio of the ellipses). The larger red ellipse significantly overlaps the black ellipse and is discarded.

probability in each topic after an initial run of pLSA. To avoid trivial doublets (those with both words in the same location), we discard those pairs of ellipses with significant overlap. We then consider all pairs of the remaining words that are within 4 nearest neighbor words of each. For scale-invariance, we scale the distances between word pairs by their relative sizes, multiplying the distance by the ratio of the larger of the two ellipse major axes over the smaller. Figure 2 shows the geometry and formation of the doublets.

**Model learning:** For pLSA, the EM algorithm is initialized randomly, typically converges in 100-300 iterations, and takes about 10 mins to run on 3K images (Matlab implementation on a 2GHz PC).

**Baseline method: Gaussian Mixture Model:** To understand the contributions of the topic discovery model to the system performance, we also implemented an algorithm with the same visual word local appearance descriptors, but without the final statistical machinery. This comparison algorithm looks for clusters of our local appearance descriptors. Using EM, we fit the distribution of word histograms over documents with mixture of  $k$  Gaussians, where  $k$  was the number of assumed topics. This model allows for multiple topics per image, but treats the histograms as generic observations rather than as word frequency distributions.

## 4. Experiments

Given a collection of unlabelled images, our goal is to automatically discover/classify the visual categories present in the data and localize them in the image. To understand how the algorithms perform, we train on image collections for which we know the desired visual topics.

We investigate three areas: (i) topic discovery – where categories are discovered by pLSA clustering on all available images, (ii) classification of unseen images – where topics corresponding to object categories are learnt on one

set of images, and then used to determine the object categories present in another set, and (iii) object detection – where we also wish to determine the location and approximate segmentation of in each image.

We use two datasets of objects, one from Caltech [?] and the other from MIT [?]. The Caltech datasets depict one object per image. The MIT dataset depicts multiple object classes per image, and includes ground truth labeling for where many of the objects are. We report results for the three areas first on the Caltech images, and then in section 4.4 show their application to the MIT images.

**Caltech image data sets** Our data set consists of images of five categories from the Caltech 101 datasets (as previously used by Fergus *et al.* [6] for supervised classification). The categories and their number of images are: faces, 435; motorbikes, 800; airplanes, 800; cars rear, 1155; background, 900. The reason for picking these particular categories is pragmatic: they are the ones with the greatest number of images per category. All images have been converted to grayscale before processing. Otherwise they have not been altered in any way, with one notable exception: a large number of images in the motorbike category (2) and airplane category (3) have a white border around the image which we have removed since it was providing an artifactual cue for object class.

#### 4.1. Topic discovery

In each experiment images are pooled from a number of original datasets, and the pLSA and baseline models are fitted to the ensemble of images (with no knowledge of the image’s labels) for a specified number of topics,  $K$ . For example, in experiment (1) the images are pooled from four categories (airplanes, cars, faces and motorbikes) and models with  $K = 4$  objects (topics) are fitted. In the case of pLSA, the model determines the mixture coefficients  $P(z_k|d_j)$  for each image (document)  $d_j$  (where  $z \in \{z_1, z_2, z_3, z_4\}$  for the four topics). An image  $d_j$  is then classified as containing object  $k$  according to the maximum of  $P(z_k|d_j)$  over  $k$ . This is essentially a one against many (the other categories) test. Since here we know the object instances in each image, we use this information as a performance measure. A confusion matrix is then computed for each experiment. The results are summarized in figure 3.

##### (1) Images of four object categories with cluttered backgrounds.

The four Caltech categories have cluttered backgrounds and significant scale variations (in the case of cars rear). An interesting observation comes from varying the number of topics,  $K$ . In the case of  $K = 4$ , we discover the four different categories in the dataset with very high accuracy (see figure 3). In the case of  $K = 5$ , the car dataset

Ex	Categories	K	pLSA		Texture	
			%	#	%	#
(1)	4	4	98	70	72	1060
(2)	4 + bg	5	78	931	73	1174
(2)*	4 + bg	6	76	1072	–	–
(2)*	4 + bg	7	83	768	–	–
(2)*	4 + bg-fxd	7	93	238	–	–

Figure 3: Summary of the experiments. Column ‘%’ shows the classification accuracy measured by the average of the diagonal of the confusion matrix. Column ‘#’ shows the total number of misclassifications. See text for a more detailed description of the experimental results. In the case of (2)\* the two/three background topics are classified as one category.

splits into two subtopics. This is because the data contains sets of many repeated images of the same car. Increasing  $K$  to 6 splits the motorbike data into sets with a plain background and cluttered background. Increasing  $K$  further to 7 and 8 ‘discovers’ two more sub-groups of car data containing again other repeated images of the same/similar cars.

It is also interesting to see the visual words which are most probable for an object, by selecting those with high topic specific probability  $P(w_i|z_k)$ . These are shown for the pLSA model for the case of  $K = 4$  in figure 4. Thus, for these four object categories, topic discovery analysis cleanly separates the images into object classes, with reasonable behavior as the number of topics increases beyond the number of objects. The most likely words for a topic appear to be semantically meaningful regions.

##### (2) Images of four object categories plus “background” category.

Here we add images of an explicit “background” category (indoor and outdoor scenes around Caltech campus) to the above experiment (1). The reason for adding these additional images is to give the methods the opportunity of discovering background “objects”.

The confusion tables as  $K$  is varied are shown as images in figure 5. It is evident, for example, that for pLSA the first topic confuses faces and backgrounds to some extent. The case of  $K = 7$  with three topics allocated to the background gives the best performance.

In the case of many of the Caltech images there is a strong correlation of the foreground and backgrounds (e.g. the faces are generally against an office background). This means that in the absence of other information the learnt topic (for faces for example) also includes words for the background. In classification, then, some background images are erroneously classified as faces. If the background distributions were to be fixed, then when determining the new topics the foreground/backgrounds are decorrelated because the backgrounds are entirely explained by the fixed topics, and the foreground words would then need to be explained by a new topic.

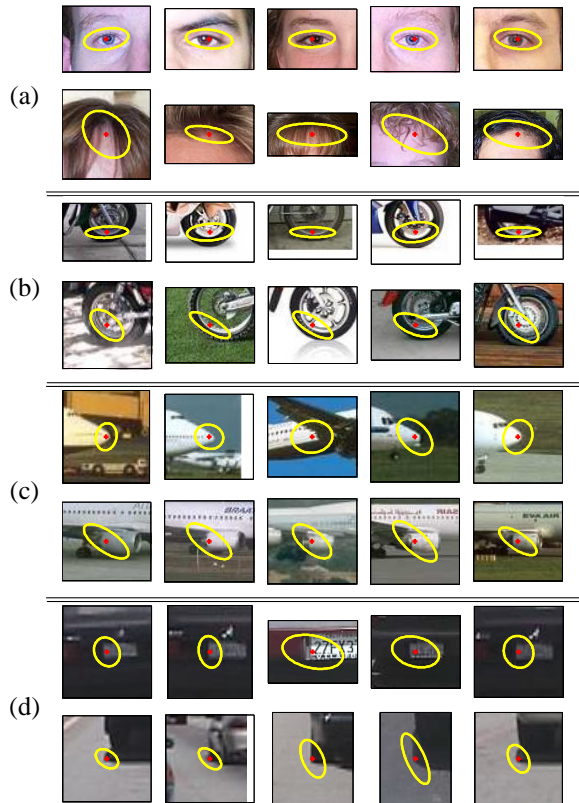


Figure 4: Two most likely words (shown by 5 examples in a row) for four learnt topics in experiment (2): (a) Faces, (b) Motorbikes, (c) Airplanes, (d) Cars.

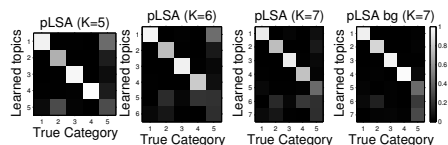


Figure 5: Confusion tables for pLSA for increasing number of topics ( $K=5,6,7$ ) and pLSA with 7 topics and fixed background respectively. Brightness indicates number. The ideal is bright down the diagonal. Note how the background (category 5 splits into 2 and 3 topics (for  $K=6$  and  $7$  respectively) and that some amount of the confusion between categories and background is removed.

Motivated by the above, we now carry out a variation in the learning where we first learn three topics on a separate set of 400 background images alone. This background set is disjoint from the one used in experiment (2). These topics are then frozen, and a pLSA decomposition with seven topics (four to be learnt, three fixed) again determined for experiment (2). The confusion table classification results are given in figure 7. It is evident that the performance is improved over not fixing the background topics above.

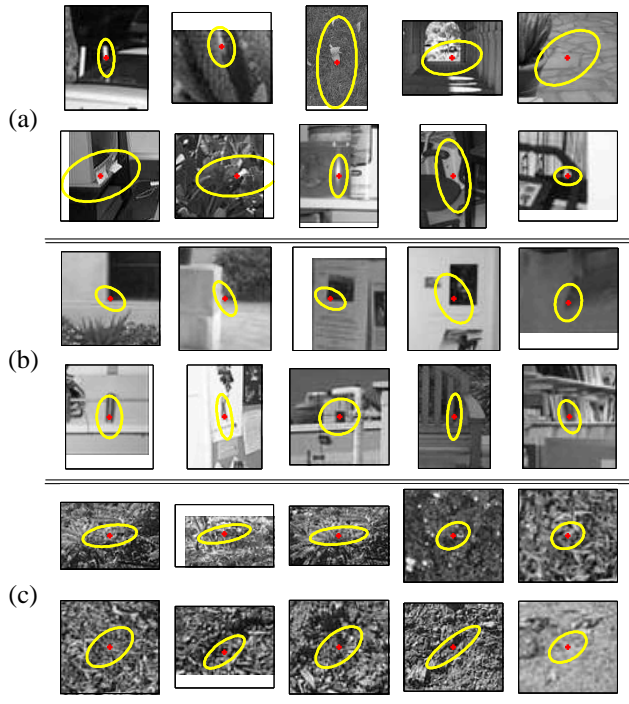


Figure 6: Two most likely words (shown by 5 examples in a row) for the three background topics learned in experiment E: (a) topic 2, mainly local feature-like structure (b) topic 4, mainly corners and edges coming from the office/building scenes, (c) topic 5, mainly textured regions like grass and trees. For topic numbers refer to figure 10(c).

True Class $\rightarrow$	Faces	Moto	Airp	Cars	Backg
Topic 1 - Faces	94.02	0.00	0.38	0.00	1.00
Topic 2 - Motorb	0.00	83.62	0.12	0.00	1.25
Topic 3 - Airplan	0.00	0.50	95.25	0.52	0.50
Topic 4 - Cars rear	0.46	0.88	0.38	98.10	3.75
Topic 5 - Bg I	1.84	0.38	0.88	0.26	41.75
Topic 6 - Bg II	3.68	12.88	0.88	0.00	23.00
Topic 7 - Bg III	0.00	1.75	2.12	1.13	28.75

Figure 7: Confusion table for experiment (3) with three background topics fixed. The sum of the diagonal (counting the three background topics as one) is 92.9%. The total number of misclassified images is 238.

**Discussion:** In the experiments it was necessary to specify the number of topics  $K$ , however Bayesian [17] or minimum complexity methods [2] can be used to infer the number of topics implied by a corpus.

## 4.2. Classifying new images

The learned topics can also be used for classifying new images, a task similar to the one in Fergus *et al.* [6]. In the case of pLSA, the topic specific distributions  $P(w|z)$  are

True Class →	Faces	Motorb	Airplan	Cars rear
Topic 1 - Faces	99.54	0.25	1.75	0.75
Topic 2 - Motorb	0.00	96.50	0.25	0.00
Topic 3 - Airplan	0.00	1.50	97.50	0.00
Topic 4 - Cars rear	0.46	1.75	0.50	99.25

Figure 8: Confusion table for unseen test images in experiment (3). Note there is very little confusion between different categories. See text.

learned from a separate set of ‘training’ images. When observing a new *unseen* ‘test’ image, the document specific mixing coefficients  $P(z|d_{test})$  are computed using the ‘fold-in’ heuristic described in [7]. In particular, the unseen image is ‘projected’ on the simplex spanned by learned  $P(w|z)$ , i.e. the mixing coefficients  $P(z_k|d_{test})$  are sought such that the Kullback-Leibler divergence between the measured empirical distribution  $\hat{P}(w|d_{test})$  and  $P(w|d_{test}) = \sum_{k=1}^K P(z_k|d_{test})P(w|z_k)$  is minimized. This is achieved by running EM in a similar manner to that used in learning, but now only the coefficients  $P(z_k|d_{test})$  are updated in each M-step. The learned  $P(w|z)$  are kept fixed.

**(3) Training images of four object categories plus “background” category.** To compare performance with Fergus *et al.* [6], experiment (2) was modified such that only the ‘training’ subsets for each category (and all background images) from [6] were used to fit the pLSA model with 7 topics (four object topics and three background topics). The ‘test’ images from [6] were then ‘folded in’ as described above. For example in the case of motorbikes the 800 images are divided into 400 training and 400 test images. In the first test the confusion between different object categories is examined. Each test image is assigned to object topic  $k$  with maximum  $P(z_k|d_{test})$  (background topics are ignored here). The confusion table is shown in figure 8. [\*\*\* we need to recite what Robs numbers were for these diagonals, and to reflect on how good this is. or is that done later? \*\*\*]]

**(4) Binary classification of category against background.** Up to this point the classification test has been one against many. In this test we examine performance in classifying (unseen) images against (unseen) background images. The pLSA model is fitted to training subsets of each category and a training subset of only 400 (out of 900) background images. Testing images of each category and testing background images are ‘folded-in’. The mixing proportion  $P(z_k|d_{test})$  for topic  $k$  across the testing images  $d_{test}$  (i.e. a row in the landscape matrix  $P(z|d)$  in figure 1b) is then used to produce a ROC curve for the topic  $k$ . Equal error rates for the four object topics are reported in figure 9.

Object categ.	pLSA (a)	pLSA (b)	Fergus <i>et al.</i> [6]
Faces	5.3	3.3	3.6
Motorbikes	15.4	8.0	6.7
Airplanes	3.4	1.6	7.0
Cars rear*	21.4 / 11.9	16.7 / 7.0	9.7

Figure 9: \*\* add fixed backgrounds here as well \*\* Equal error rates for image classification task for pLSA and the method of [6]. Test images of a particular category were classified against (a) testing background images (test performed in [6]) and (b) testing background images *and* testing images of all other categories. The improved performance in (b) is because our method exhibits very little confusion between different categories. (\*) The two performance figures correspond to training on 400 / 900 background images respectively. In both cases, classification is performed against an unseen test set of road backgrounds (as in [6]), which was folded-in. See text for explanation.

Note that for Airplanes and Faces our performance is similar to that of [6] despite the fact that our ‘training’ is unsupervised in the sense that the identity of the object in an image is *not known*. This is in contrast to [6], where each image is labelled with an identity of the object it contains, i.e. about  $5 \times 400$  items of supervisory data vs. one label (the number of topics) in our case.

In the case of motorbikes we perform worse than [6] mainly due to confusion between motorbike images containing textured background and textured background topic. The performance on Cars rear is poor because Car images are split between two topics in training (a similar effect happens in experiment D for  $K=6$ ). This splitting can be avoided by including more background images. In order to make results comparable with [6], Cars rear images were classified against completely new background dataset containing mainly empty roads. This dataset was not seen in the learning stage and had to be ‘folded-in’ which makes the comparison on Cars rear slightly unfair to the topic discovery approach.

### 4.3. Segmentation

In this section we evaluate the image’s spatial segmentation that have been discovered by the model fitting. As a first thought, it is absurd that a bag of words model could possibly have anything useful to say about image segmentation, since all spatial information has been thrown away. However, the pLSA model delivers the posteriors

$$P(z_k|w_i, d_j) = \frac{P(w_i|z_k)P(z_k|d_j)}{\sum_{l=1}^K P(w_i|z_l)P(z_l|d_j)}, \quad (3)$$

and consequently for a word occurrence in a particular document we can examine the probability of different topics.

Figure 10 shows examples of ‘topic segmentation’ induced by  $P(z_k|w_i, d_j)$  for the case of experiment (2) with



Topic	$P(\text{topic} \text{image})$	# regions
1 Motorbikes (green)	0.07	1
2 Backg I (magenta)	0.09	1
3 Face (yellow)	0.48	128
4 Backg II (cyan)	0.17	12
5 Backg III (blue)	0.15	23
6 Cars (red)	0.03	0
7 Airplane (black)	0.00	0

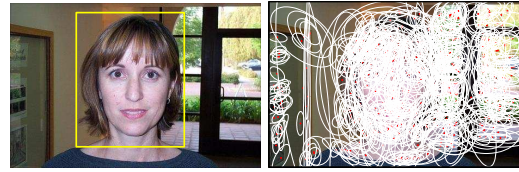
(c)

Figure 10: Image as a mixture of visual topics (Experiment (2)) - I. (a) Original frame. (b) Image as a mixture of a face topic (yellow) and background topics (blue, cyan). Only elliptical regions with topic posterior  $P(z|w, d)$  greater than 0.8 are shown. In total 7 topics were learned for this dataset which contained (faces, motorbikes, airplanes, cars, and background images). The other topics are not significantly present in the image since they mostly represent the other categories and other types of background. Table (c) shows the mixture coefficients  $P(z|d)$  for this particular image. In total there are 693 elliptical regions in this image of which 165 (102 unique visual words) have  $P(z|w, d)$  above 0.8 (those shown in (b)).

7 topics. In particular, we show only visual words with  $P(z_k|w_i, d_j)$  greater than 0.8. There is an impressive alignment of the words with the corresponding object areas of the image. Note the words shown are not simply those most likely for that topic. Rather, from (3), they have high probability of that topic *in this image*. This is an example of overcoming polysemy – the probability of the particular word depends not only on the probability that it occurs within that topic (face, say) but also on the probability that the face topic has for that image, i.e. the evidence for the face topic from other regions in the image.

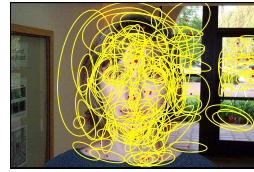
**(5) Image segmentation for faces** Improving segmentation by local co-occurrences of visual words. Figure 11 compares segmentation on one example image of a face using singlets and doublets. Procedure is: learn background topic as in experiment (2). Learn pLSA decomposition for all training faces and training background \*\* yes ? \*\* with fixed background topics. Doublet vocabulary is then formed from the top 100 visual words of the face topic. pLSA decomposition is learned again for the combined vocabulary of singlets and doublets with the background topics fixed. The reason for running the first level singleton pLSA is to reduce the doublet vocabulary size to a manageable size.

Note the level of supervision to achieve this segmenta-

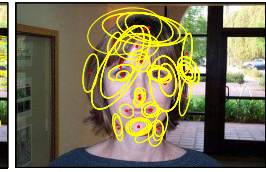


a

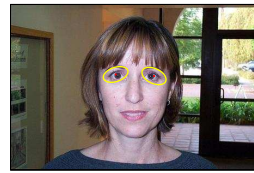
b



c



d



e



f

Figure 11: Improving object segmentation. (a) The original frame with ground truth bounding box. (b) All 601 detected elliptical regions superimposed on the image. (c) Segmentation obtained by pLSA on single regions (d) Segmentation obtained using localized spatial co-occurrences of pairs of regions. Note the extra regions on the right-hand side background of (c) are removed in (d). (e) and (f) show examples of locally co-occurring regions.

tion: the images are an unordered mix of faces and backgrounds. It is not necessary to label which is which at any stage, yet both the face images *and their segmentation* are learnt.

Comparison with ground truth segmentation: The segmentation is assessed on a set of 217 face images with known bounding boxes. The performance score is the percentage of regions which fall inside the bounding box. Singleton segmentation score: 77.02% (Face specific doublets) Doublet segmentation: 94.1% If doublets are formed from top 40 visual words across all topics (including background topics) the segmentation score drops to 92.7%.

#### 4.4. MIT image dataset results

**MIT image data sets** \*\* Number of images, stats on object categories etc \*\*. The MIT dataset contains 2873 images of outdoor and indoors scenes. with annotated objects. We consider the following 16 object categories which have more 200 labelled instances:

Again all images have been converted to grayscale before processing.

**Topic discovery and classification** \*\* Here put topic discovery,  $K = 2, 10$  for MIT. \*\*



Figure 12: pLSA on the MIT dataset for (a)  $K = 2$  and (b)  $K = 10$ . Each topic is shown by a row of 10 images (resized to squares). The images are a random sample from the top 100 most probable images for each topic.

Here we fit pLSA/LDA with  $K$  topics to the entire dataset. The topic discovery is shown for  $K = 2$  and 10. For  $K = 2$  the images are mainly split into indoor and outdoor scenes. For  $K = 10$  the equal error rates are reported in table ???. Note that several objects might be covered by the same topic, e.g. (a mouse, a keyboard, and a screen) have best equal error rates for the same topic (10). Ten images for each discovered topic are shown in figure 12.

The MIT data set can have multiple objects in an image e.g. a tree and a building. Therefore we do not perform classification to the topic with a maximal weight. Instead we compute an ROC curve for each category and a report a topic with minimal equal error rate. This shows how well the different categories are covered by the discovered topics.

**Segmentation of the mixed category images** Procedure is: Learn pLSA decomposition for 10 topics; form doublets from top 50 pLSA words for each topic (\*\* ?= how many doublets \*\*); relearn pLSA for 10 topics for new vocabulary consisting of all singlets and all doublets. Figure 13 shows only the (top?) doublets for each topic.



Figure 13: Example segmentations on the MIT dataset for 10 topic decomposition. (a) the original image. (b) all detected regions superimposed (c) the topic induced segmentation. Note each image is segmented into several ‘topics’.

## 5. Conclusions

1. We have demonstrated that it is possible to learn visual object classes simply by looking; we identify the object categories for each image with the high reliabilities shown in figure 3, using a corpus of unlabelled images.
2. Using these learnt topics for classification, we reproduce the experiments (training/testing) of [6], and obtain very competitive performance – despite the fact that [6] had to provide about  $400\times$  number of classes supervisory labels, and we provide one label.
3. Using visual words with the highest posterior probabilities for each object correspond fairly well to the spatial locations of each object. This is rather remarkable considering our use of the bag of words model.
4. By introducing a second vocabulary built on spatial co-occurrences of word pairs, cleaner and accurate

segmentations are achieved. These enable object *detection*, rather than simply classification.

5. What's next ?

## References

- [1] K. Barnard, P. Duygulu, N. de Freitas, D. Forsyth, D. Blei, and M. Jordan. Matching words and pictures. *Journal of Machine Learning Research*, 3:1107–1135, 2003.
- [2] A. R. Barron and T. M. Cover. Minimum complexity density estimation. *IEEE Trans. on Information Theory*, 4:1034–1054, 1991.
- [3] D. Blei, A. Ng, and M. Jordan. Latent dirichlet allocation. *Journal of Machine Learning Research*, 3:993–1022, 2003.
- [4] G. Csurka, C. Bray, C. Dance, and L. Fan. Visual categorization with bags of keypoints. In *Workshop on Statistical Learning in Computer Vision, ECCV*, pages 1–22, 2004.
- [5] P. Duygulu, K. Barnard, J. F. G. de Freitas, and D. A. Forsyth. Object recognition as machine translation: Learning a lexicon for a fixed image vocabulary. In *Proc. ECCV*, 2002.
- [6] R. Fergus, P. Perona, and A. Zisserman. Object class recognition by unsupervised scale-invariant learning. In *Proc. CVPR*, 2003.
- [7] T. Hofmann. Probabilistic latent semantic indexing. In *SI-GIR*, 1999.
- [8] T. Hofmann. Unsupervised learning by probabilistic latent semantic analysis. *Machine Learning*, 43:177–196, 2001.
- [9] D. Lowe. Object recognition from local scale-invariant features. In *Proc. ICCV*, pages 1150–1157, 1999.
- [10] J. Matas, O. Chum, M. Urban, and T. Pajdla. Robust wide baseline stereo from maximally stable extremal regions. In *Proc. BMVC.*, pages 384–393, 2002.
- [11] K. Mikolajczyk and C. Schmid. An affine invariant interest point detector. In *Proc. ECCV*. Springer-Verlag, 2002.
- [12] A. Opelt, A. Fussenegger, and P. Auer. Weak hypotheses and boosting for generic object detection and recognition. In *Proc. ECCV*, 2004.
- [13] F. Schaffalitzky and A. Zisserman. Multi-view matching for unordered image sets, or “How do I organize my holiday snaps?”. In *Proc. ECCV*, volume 1, pages 414–431. Springer-Verlag, 2002.
- [14] H. Schneiderman and T. Kanade. A statistical method for 3D object detection applied to faces and cars. In *Proc. CVPR*, 2000.
- [15] J. Sivic and A. Zisserman. Video Google: A text retrieval approach to object matching in videos. In *Proc. ICCV*, 2003.
- [16] F. Souvannavong, B. Merialdo, and B. Huet. Improved video content indexing by multiple latent semantic analysis. In *Proc. CIVR*, 2004.
- [17] Y. W. Teh, M. I. Jordan, M. J. Beal, and D. M. Blei. Hierarchical dirichlet processes. In *Proc. NIPS*, 2004.
- [18] <http://www.robots.ox.ac.uk/~vgg/research/affine/>.
- [19] P. Viola and M. Jones. Rapid object detection using a boosted cascade of simple features. In *Proc. CVPR*, 2001.
- [20] M. Weber, M. Welling, and P. Perona. Unsupervised learning of models for recognition. In *Proc. ECCV*, pages 18–32, 2000.
- [21] R. Zhang and Z. Zhang. Hidden semantic concept discovery in region based image retrieval. In *Proc. CVPR*, 2004.